Nuclear Engineering and Design 289 (2015) 117–125

Contents lists available at ScienceDirect

Nuclear Engineering and Design

journal homepage: www.elsevier.com/locate/nucengdes

Passive safety system of a super fast reactor

Sutanto[a,b,*], Yoshiaki Oka[c]

[a] Cooperative Major in Nuclear Energy, Waseda University, Tokyo, Japan
[b] Polytechnic Institute of Nuclear Technology—National Nuclear Energy Agency, Yogyakarta, Indonesia
[c] The University of Tokyo, Tokyo, Japan

HIGHLIGHTS

- Passive safety system of a Super FR is proposed.
- Total loss of feedwater flow and large LOCA are analyzed.
- The criteria of MCST and core pressure are satisfied.

ARTICLE INFO

Article history:
Received 25 August 2014
Received in revised form 6 April 2015
Accepted 8 April 2015

ABSTRACT

Passive safety systems of a Super Fast Reactor are studied. The passive safety systems consist of isolation condenser (IC), automatic depressurization system (ADS), core make-up tank (CMT), gravity driven cooling system (GDCS), and passive containment cooling system (PCCS). Two accidents of total loss of feedwater flow and 100% cold-leg break large LOCA are analyzed by using the passive systems and the criteria of maximum cladding surface temperature (MCST) and maximum core pressure are satisfied. The isolation condenser can be used for mitigation of the accident of total loss of feedwater flow at both supercritical and subcritical pressures. The ADS is used for depressurization leading to a loss of coolant during line switching to operation of the isolation condenser at subcritical pressure. Use of CMT during line switching recovers the lost coolant. In case of large LOCA, GDCS can be used for core reflooding. Coolant vaporization in the core released to containment through the break is condensed by passive containment cooling system. The condensate flows to the GDCS pool by gravity force. The maximum cladding surface temperature (MCST) of the accident satisfies the criterion.

1. Introduction

A supercritical pressure water-cooled reactor (SCWR) is one of the six Generation-IV reactors developed recently throughout the world. It is developed based on the technologies of simplified light water reactors (LWRs) and supercritical thermal power plants. It uses once through direct cycle of cooling system operating at supercritical pressure. High outlet temperature and low coolant flow rate improve its efficiency and economy. In Japan, research and development of SCWR have been conducted since 1989 at the University of Tokyo and Waseda University. The concept designs are called as super light water reactor (Super LWR) and super fast reactor (Super FR) (Oka et al., 2010). The Super FR is the fast version of the Super LWR. Currently, analysis of the influences of thermal correlations on neutronic–thermohydraulic coupling calculation of SCWR has been conducted in China (Xu et al., 2015).

A Super FR is designed to find a way of competitive plutonium utilization. It has higher power density than that of a Super LWR leading to an improvement of its economy. Three core designs of Super FRs have been carried out to improve the core structures by simplification. Early design was a two-flow pass core of a Super FR with downward-upward flow as shown in Fig. 1(a) (Yoo et al., 2006). Unfortunately, flow stagnation occurred during loss of coolant flow events due to buoyancy effect in the downward channel, which leaded to fuel heat-up (Oka et al., 2011; Zhu et al., 2013). The downward flow in the first pass also made the upper core structure to be complex. To address these issues a two-flow pass core of a Super FR with all upward flow was designed as shown in Fig. 1(b) (Liu and Oka, 2013a). However, the structures of lower and gap plenums were still complex due to seals between hot and cold coolant in the upstream of fuel assemblies. Besides, the control rod only put in the second pass due to structure of upper mixing

---

* Corresponding author. Present address: Polytechnic Institute of Nuclear Technology-National Nuclear Energy Agency, Jl. Babarsari PO BOX 6101/YKBB, Yogyakarta 55281, Indonesia.

E-mail addresses: sutanto@fuji.waseda.jp, sutanto5381@batan.go.id (Sutanto).

http://dx.doi.org/10.1016/j.nucengdes.2015.04.029

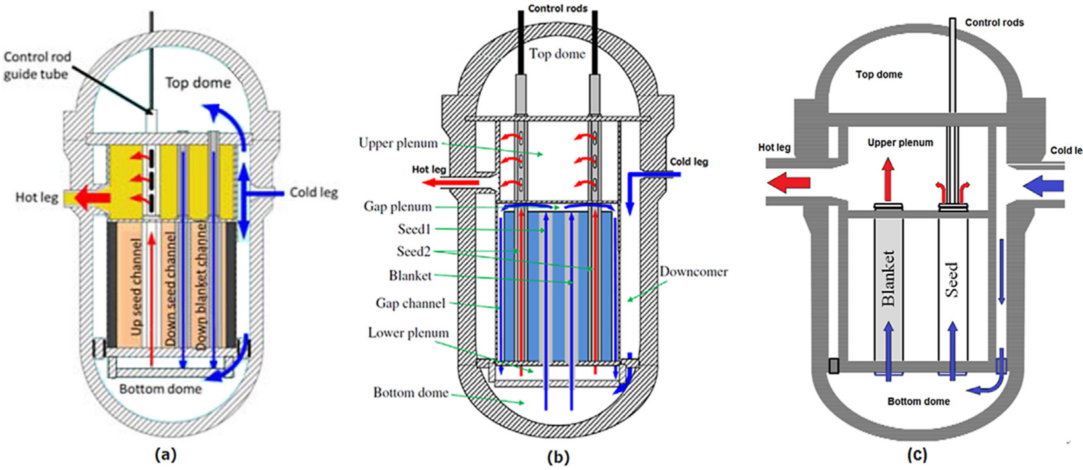

Fig. 1. Development of Super FRs: (a) two-flow pass core with downward-upward flow, (b) two-flow pass core with all upward flow, (c) single flow pass core with all upward flow.

plenum above the first pass. To simplify refueling and the structure of the plenums, a single-flow pass core of a Super FR has been designed as shown in Fig. 1(c) (Liu and Oka, 2013b, 2015). For its safety, zirconium hydride (ZrH) layer was applied in the blanket assembly to attain a negative void reactivity (Oka and Jevremovic, 1996; Cao et al., 2008).

Safety analysis is an important issue in core designs. Since a Super FR uses once through direct cycle operating at supercritical pressure, its safety characteristics are different from that of LWRs. There is no water level at supercritical pressure. The fundamental safety requirementis maintaining the core coolant flow rate instead of keeping the water (Ishiwatari et al., 2005a).

Safety analyses of the Super FRs were already carried out in the past studies (Ikejiri et al., 2010; Li et al., 2013; Sutanto and Oka, 2014). However, the safety analyses relied on active safety systems. Passive safety systems of the Super FRs were not studied yet. Safety analyses of the Super FRs based on passive safety system were not carried out yet as well.

Safety analysis of a thermal spectrum SCWR with passive safety systems was reported (MacDonald et al., 2005; Wu et al., 2012). The power density of the Super FR is higher than the thermal spectrum SCWR. It is necessary to study the passive safety system for the Super FR with single flow pass core, the latest design.

Safety analysis of the Super FR in our past studies showed that a total loss of feedwater flow and LOCA accidents were important due to immediate loss of core coolant flow (Ikejiri et al., 2010; Li et al., 2013; Sutanto and Oka, 2014). The accident of total loss of feedwater flow was mitigated by driving the core coolant flow rate through auxiliary feedwater systems (AFS) at supercritical pressure, while at subcritical pressure, low pressure coolant injection systems (LPCI) were used for reflooding. In fact, operation of both safety systems which were driven by pumps relied on the availability of emergency power (Ishiwatari et al., 2005a). Emergency power dependence limits the reliability of the safety systems. Long grace period for the pumps and reducing maintenance burden of the safety system are attractive for the passive safety system. This study present the safety analysis of a Super FR with single flow pass core based on the passive safety system.

2. Core feature of the Super FR with single flow pass

Safety of a single-flow pass core is analyzed in this study due to its simplest structure of the Super FRs as shown in Fig. 1(c). It might be the candidate for construction in the future. Characteristics of the core design are shown in Table 1. Fuel channel structure of the single flow pass core of Super FR consists of seed and blanket assemblies which coolant flow direction are all upward. The coolant enters the core through downcomer with inlet temperature of 280 °C and then it is distributed into seed assembly (92.3%) and blanket assembly (7.7%) by orifices. Afterwards the coolant mixes in the upper plenum and flows out through hot-leg with temperature of 500 °C.

Table 1
Core characteristics of the single flow pass core of Super FR.

Parameters	Value
Thermal/electric power (MW)	2353/1000
Pressure (MPa)	25
Inlet/outlet temperature (°C)	280/500
Active core height (m)	2.4
Number of assembly (seed/blanket)	78/37
Number of fuel rods per assembly (seed/blanket)	978/547
Total flow rate (kg/s)	1200
MCST of BOC/EOC (°C)	646/647

Layouts of the fuel assemblies are shown in Fig. 2 (Liu and Oka, 2013b). Seed assembly has a function as primary power generating source which is comprised of mixed oxide (MOX) fuel as shown in Fig. 2(a). An axial large density is introduced in the single flow pass core which in turn it leads to a high power peaking at the beginning of cycle (BOC). However, the power peaking can be adjusted by changing the Pu enrichment in the axial direction of seed assembly. Meanwhile, at the top part of blanket assembly as shown in Fig. 2(b), Pu building-up due to fuel breeding in the UO_2 zones introduces large power rise which increases the outlet coolant temperature at end of cycle (EOC). To address this problem, some MOX fuel is also applied at the bottom part of blanket assembly as shown in Fig. 2(c) to mitigate the large power rise. ZrH rods are applied surrounding the breeding region to attain negative void reactivity during flow abnormality. It acts as inherent passive safety characteristic of the Super FR. Some SUS (steel use stainless/stainless steel) rods are arranged at the peripheral region of the blanket assembly to reduce pin-power peaking induced by the ZrH to the neighboring seed. Power distribution of the Super FR is shown in Fig. 3 (Liu and Oka, 2013b).

3. Plant and passive safety system

Since a Super FR is developed based on proven technologies of LWRs, its passive safety systems are also developed by referring to the passive safety systems of PWR (AP1000) and BWR (ESBWR)

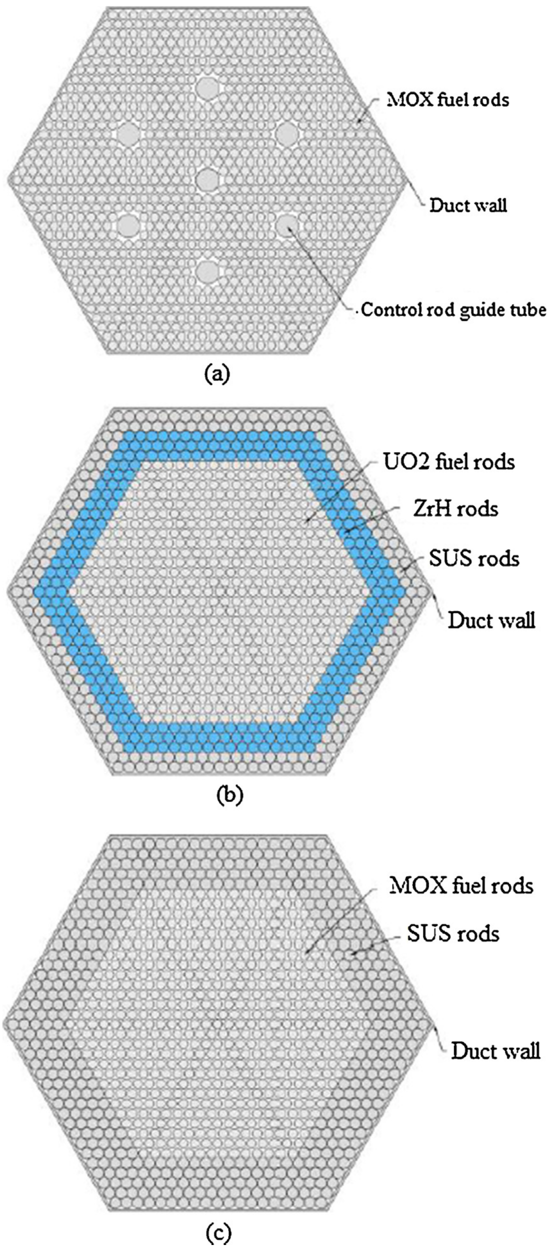

Fig. 2. Layouts of fuel assemblies: (a) seed assembly, (b) top side of blanket assembly, (c) bottom side of blanket assembly.

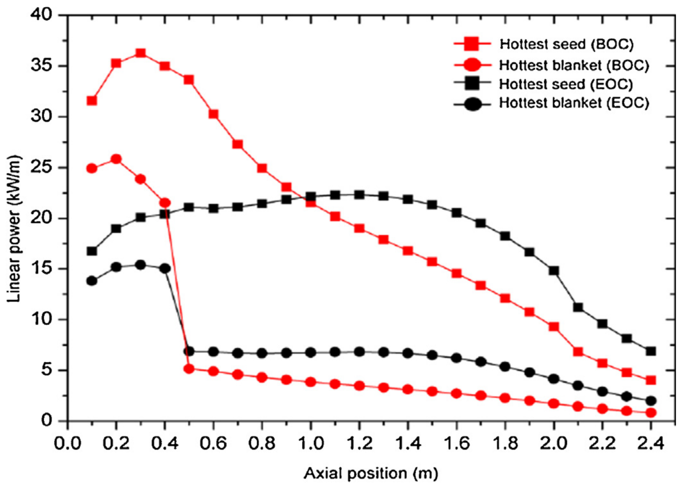

Fig. 3. Axial power distribution of the single flow pass core of Super FR.

Table 2
Actuation signal of the passive safety system.

Passive system	Actuating signal	Driving force
IC	Flow low (7%)	Density difference Pressure difference
ADS	Pressure low (23.5 MPa)	Pressure difference
CMT	Pressure low (7 MPa)	Gravity
GDCS	Pressure low (0.15 MPa)	Gravity
PCCS	Containment pressure high	Pressure difference

(Cummins et al., 2003; Xu et al., 2004). Passive safety systems of the reactors have functions to establish and maintain core cooling and containment integrity through core residual heat removal, depressurization, safety injection and passive containment cooling system. Both subcritical reactors of AP1000 and ESBWR use condensers for passive residual heat removal from the core and containment. Besides low pressure coolant injection from water storage tank, an AP1000 uses core make-up tanks and accumulators for core coolant injection at high pressure due to its higher operating pressure than ESBWR. Some stages of automatic depressurization system depressurize the core pressure before coolant injection from the water storage tank at low pressure.

Similar to that of LWRs, passive safety systems of a Super FR consist of isolation condensers (IC), automatic depressurization system (ADS), core make-up tank (CMT), gravity driven cooling system (GDCS) and passive containment cooling system (PCCS). Use of the IC, GDCS and PCCS refers to that of ESBWR considering the once through direct cycle, while use of the CMT refers to that of AP1000 considering the high operating pressure. Even though the passive safety systems are similar, the passive safety characteristics of a Super FR are, however, different from that of AP1000 and ESBWR because the operating pressure of a Super FR is at supercritical pressure (25 MPa). Besides, the water inventory in the RPV is much less than that of the LWRs. The safety principle is by keeping the core coolant flow rate at supercritical pressure instead of keeping the water level at subcritical pressure of the LWRs (Ishiwatari et al., 2005a). Hence, main function of the passive safety systems of a Super FR is to keep its core coolant flow rate in case of abnormality.

Emergency condensers (EC) which is installed online is also analyzed referring to the emergency condensers of KERENA (Zacharias et al., 2012). In case of total/partial loss of feedwater flow rate, it is expected to have immediate mitigation due to no valve applied along the condenser line. Any emergency power is not necessary.

Some passive safety systems of thermal SCWRs have also been proposed (MacDonald et al., 2005; Wu et al., 2012). However, the power density of a Super Fast Reactor is higher than that of the thermal SCWRs. Mitigation of abnormalities in a Super FR is more challenging than that in both LWRs and thermal SCWRs due to less water inventory in the RPV of the Super FR. The passive safety characteristics of a Super FR might be different from that of the SCWRs. The plant and passive safety system concept of the Super FR is shown in Fig. 4. Actuation levels of the safety system are determined conservatively and shown in Table 2.

3.1. Isolation condenser (IC)

Isolation condenser is applied for core heat removal in case of non-LOCA accidents. Inlet of the IC is connected to the hot-leg through a steam line with normally open, while the outlet of IC is connected to downcomer through a drain line by direct vessel injection with normally closed. At normal operation, the condenser tubes are submerged with cold water which acts as out-vessel

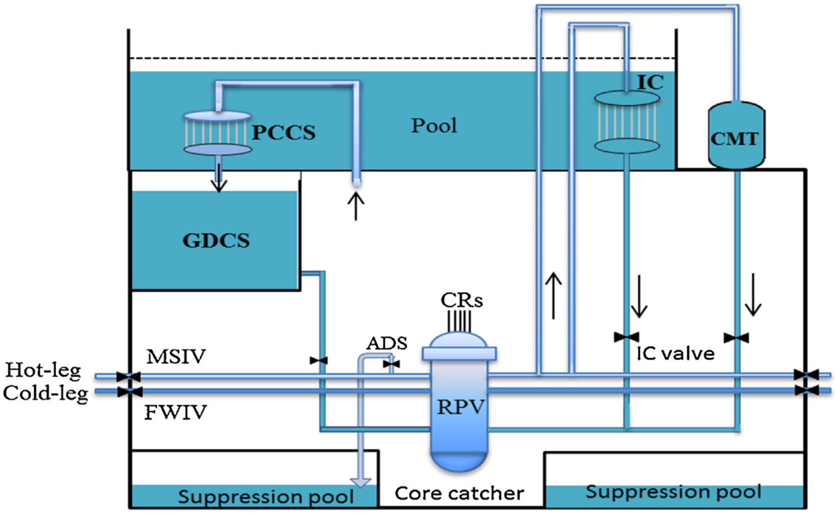

Fig. 4. Passive safety system of the single flow pass core of Super FR.

water inventory. Temperature of the cold water is assumed to be the same as condenser pool temperature which is placed outside of the containment. Flow low 7% is chosen conservatively as the signal actuation of the IC. After IC actuation, cold water in the drain line will flows immediately to the core due to potential of hydrostatic pressure. Coolant heat-up in the core enlarges the density difference between the coolant in the drain line and the coolant in the core which in turn might generate a natural flow rate.

3.2. Automatic depressurization system (ADS)

The function of ADS is to induce core coolant flow during depressurization (Ishiwatari et al., 2005a). Large core coolant flow rate is generated passively due to large pressure difference between the reactor pressure vessel (RPV) and the suppression pool. Pressure of the suppression pool is assumed the same as containment pressure, 0.15 MPa. Pressure low 23.5 MPa is used as the actuation signal the same as that used in active safety system of a Super FR (Sutanto and Oka, 2014). Operation of the ADS leads to a loss of coolant in the RPV. In case of non-LOCA events, it might be possible to close the ADS valves and switched to the IC line when the core pressure achieves saturation pressure. The remaining water inventory in the RPV can be used for core heat removal by natural circulation through the IC at subcritical pressure. Furthermore, lost coolant due to ADS operation might be recovered by coolant injection from a core make-up tank during the line switching.

3.3. Core make-up tank (CMT)

The function of CMT is for coolant recovery during line switching from ADS to IC operation at subcritical pressure. It acts as cold coolant injection at intermediate pressure referring to accumulator of AP1000 (Cummins et al., 2003). The coolant temperature is assumed the same as room temperature, 30 °C. Low pressure of 7 MPa is used as the actuation signal which is the same as for line switching from ADS to IC lines.

3.4. Gravity driven cooling system (GDCS)

GDCS is used for core reflooding in case of LOCA accidents. It is placed inside the containment. When a LOCA accident happens, firstly ADS will be actuated by pressure low leading to decreased core pressure and lost coolant in the RPV through both the break and the ADS valves. When the core pressure is the same as containment pressure, cold coolant from GDCS will be injected by gravity force.

Table 3
Dimension of passive components.

Component	Dimension
IC	
Inner tube diameter (mm)	12
Tube length (m)	10
Tubes number	300
Total weight (kg)	3396
CMT	
Volume (m^3)	5
GDCS	
Volume (m^3)	157

3.5. Passive containment cooling system (PCCS)

PCCS is used for containment pressure mitigation. Pressure of the containment is increased due to break flow of LOCA accidents. High coolant enthalpy of break flow will be condensed in the condenser of PCCS and the condensate flow is directed to the GDCS pool by gravity force. Combination of the GDCS and the PCCS will result a long term of core cooling in case of LOCA accidents.

4. Components design and accidents analyses

4.1. Components design

Dimension of the passive system components are shown in Table 3.

4.1.1. Isolation condenser

At normal operation, the inlet of condenser is connected to steam line with normally open. Pressure of the condenser during the reactor operation is the same as operating pressure, 25 MPa. Regarding to abnormal transient events, the design pressure (P) of the IC is 27.5 MPa (Sutanto and Oka, 2014). The inner diameter and the length of a condenser tube are 12 mm and 10 m referring to those of IC of American SCWR (MacDonald et al., 2005). Material of the condenser tubes are assumed using material of SBV2 which the maximum allowable stress (S) and the material density are 135.2 MPa and 8.7 g/cm^3, respectively. To withstand with the design pressure, the tube thickness (t) is calculated by the following equation (Kataoka and Ishii, 1984).

$$t = \left(\sqrt{\frac{SE + P}{SE - P}} - 1 \right) R \tag{1}$$

Parameter E shows the efficiency which is taken as 100% and R is the inner diameter of tube. The tube thickness is 2.8 mm and the weight of one tube is 11.3 kg. If the number of tubes is 300, the total weight of the condenser tubes is 3396 kg.

4.1.2. *Core make-up tank*

Since CMT is used for coolant recovery, the minimum dimension of the CMT is the same as volume of lost coolant during ADS operation. The initial coolant mass in the RPV is about 25,000 kg. Based on the previous study of ADS operation, depressurization from 23.5 MPa to saturation pressure of about 7 MPa took time of less than 2 s. Loss of coolant within 2 s is calculated and the result is shown in Fig. 10 which is discussed later in the following section of accidents analyses. The lost coolant is estimated about 5000 kg. At water temperature of 30 °C, the water density is about 996 kg/m^3. The minimum volume of the CMT is 5 m^3.

4.1.3. *Gravity driven cooling system*

Dimension of the GDCS is calculated based on the reflooding process of the Super FR conducted in the past study (Sutanto and Oka, 2014). The reflooding process was using LPCI with constant flow injection of 600 kg/s (2 unit of LPCI) and water temperature of 30 °C. The reflooding time was 260 s considering the vaporization rate of water level in the core. The total mass of water needed for the reflooding process is 156,000 kg. So that, the minimum volume of GDCS needed to contain the water is about 157 m^3.

4.2. *Accidents analyses*

Two accidents of total loss of feedwater flow and large LOCA are analyzed by using the proposed passive safety system. The same safety criteria as those in the past studies are used in this analysis. The safety criteria are for maintaining the fuel pellet and rod integrity and pressure boundary integrity (Ishiwatari et al., 2005b). These requirements are transformed to corresponding maximum cladding surface temperature (MCST) and maximum core system pressure limitations. The MCST criterion for these accidents is 1260 °C and the maximum allowable pressure is 30.3 MPa.

A code of transient and accident analyses at supercritical and subcritical pressure (SPRAT) is modified to simulate the passive safety systems. This code had been validated for safety analyses of Super LWRs and Super FRs (Okano et al., 1996; Oka et al., 2010; Ishiwatari et al., 2005b). Firstly the calculation model of the passive safety system is developed as shown in Fig. 5. Afterwards the code is modified based on the calculation model.

Density, temperature, enthalpy, and mass flow rate in each node are calculated by solving the laws of mass, energy and momentum conservations, and state equation as follow (Oka et al., 2010):

$$\frac{\partial \rho}{\partial t} + \frac{\partial (\rho u)}{\partial z} = 0 \tag{2}$$

$$\frac{\partial (\rho h)}{\partial t} + \frac{\partial (\rho u h)}{\partial z} = \frac{P_e}{A} q'' \tag{3}$$

$$-\frac{\partial P}{\partial z} = \frac{\partial (\rho u)}{\partial t} + \frac{\partial \left(\rho u^2\right)}{\partial z} + \rho g \cos\theta + \frac{2f}{D_h} \rho u^2 \tag{4}$$

$$\rho = f(P, h) \tag{5}$$

where z is position (m), t is time (s), ρ is coolant density (kg/m^3), u is coolant velocity (m/s), h is coolant specific enthalpy (J/kg), q'' is heat flux on the rod surface (W/m^2), p is pressure, and $P_e, A, g, \theta, f, D_h$ are the parameters of heated perimeter (m), cross-sectional area of fuel channel (m^2), gravity acceleration (m/s^2), angle of inclination (°), coefficient of friction pressure drop, and hydraulic diameter of fuel channel (m), respectively.

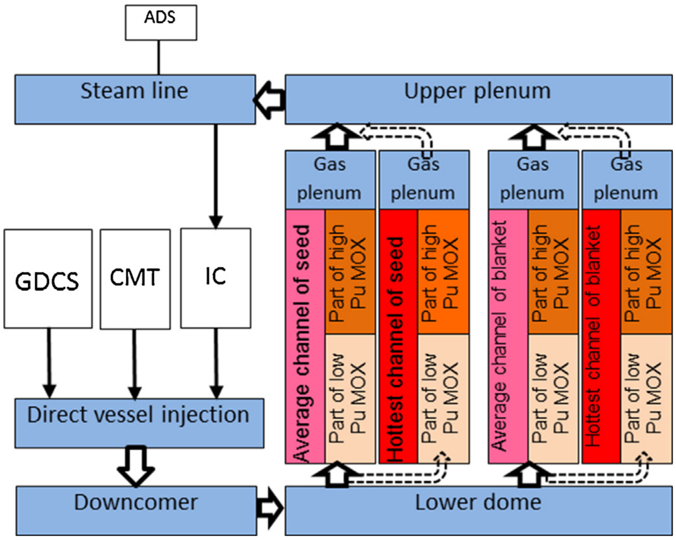

Fig. 5. Calculation model of passive safety analysis.

4.2.1. *Total loss of feedwater flow*

In an accident of total loss of feedwater flow, both reactor coolant pumps are tripped leading to a linear decrease of feedwater flow to zero within 5 s. Natural flow rate is calculated based on Eq. (6). Coolant heat up in the core enlarges the density difference between the coolant in the drain line ($\rho_{\text{drain line}}$) and the coolant in the core (ρ_{core}).

$$(\rho_{\text{drainline}} - \rho_{\text{core}}) g \times h = \Delta P_{\text{total}} \tag{6}$$

Parameters of h and g are the elevation of IC and the gravity acceleration, respectively, while theΔP_{total} is the total pressure drop along the IC loop. The pressure drop consists of pressure drops due to acceleration, elevation, friction and orifice which are expressed as in Eqs. (7) to (10) (Oka et al., 2010).

Acceleration (acc):

$$\Delta P_{\text{acc}} = \sum_i \left(\frac{\rho_i v_i^2}{2} - \frac{\rho_{i-1} v_{i-1}^2}{2} \right) \tag{7}$$

Elevation (elev):

$$\Delta P_{\text{elev}} = \rho_0 g \Delta z N - \sum_i \rho_i g \Delta z \tag{8}$$

Friction (fri):

$$\Delta P_{\text{fri}} = \sum_i 2 \left(\frac{\Delta z}{D_h} \right) \rho_i v_i^2 f_i \tag{9}$$

Orifice (ori):

$$\Delta P_{\text{ori}} = \sum_i K_{\text{ori}} \rho_i \frac{v_i^2}{2} \tag{10}$$

Variable of v is coolant velocity (m/s) and parameters of Δz, N, f, and K are mesh size, meshes number, friction pressure drop coefficient, and resistance coefficient respectively.

Natural flow rate is calculated by iteration with flow chart as shown in Fig. 6. The calculation results are shown in Fig. 7. First, reactor scram will be actuated by flow low 90% which is the same

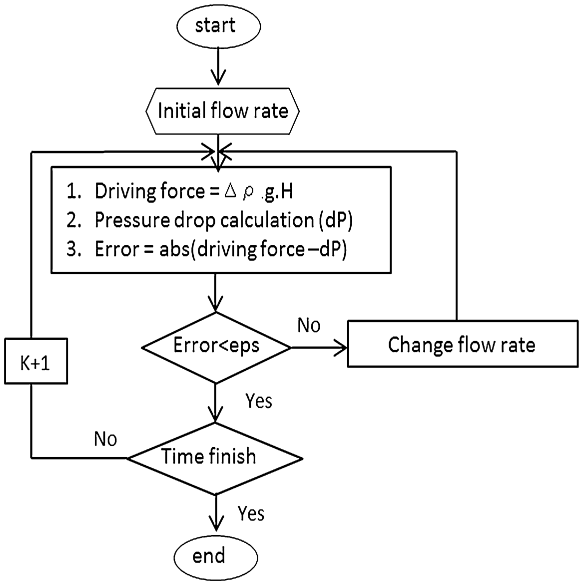

Fig. 6. Flow chart of natural flow rate calculation.

scram actuation as in the past study of a Super LWR (Ishiwatari et al., 2005a,b). The decreased feedwater flow rate leads the core pressure to decrease while the increase of MCST is due to mismatched decrease of the flow rate and the power. When the decreased feedwater flow rate reaches 7%, the IC valve is automatically opened. The core flow rate experiences a zero flow rate in a short time whenfeedwater flow rate is totally lost. The core pressure suddenly increases due to coolant heat-up in the core. However, natural flow rate is generated early due to hydrostatic pressure of the cold water in the drain line mitigating the increased pressure. The core pressure is slightly decreased due to heat removal which is effective at pseudo-critical temperature of about 385 °C along the condenser tubes. The increased MCST is also milder due to the natural flow rate and finally decreasing slightly. The core pressure continues to decrease until the pressure achieves the actuation level of ADS. Once the ADS is actuated, large core coolant flow rate is induced and the MCST will be more mitigated. The core pressure is decreased to subcritical rapidly.

Fig. 8 shows the performance of IC as function of the tubes number. Fewer tubes number leads to less effective mitigations of pressure and MCST due to less heat removal in the condenser. Tubes number of 200 leads a small natural flow rate due to small coolant density difference. The pressure continues to increase rapidly due to coolant heat-up and the MCST also increases slightly. Tubes number of more than 300 is able to mitigate the increased pressure and MCST.

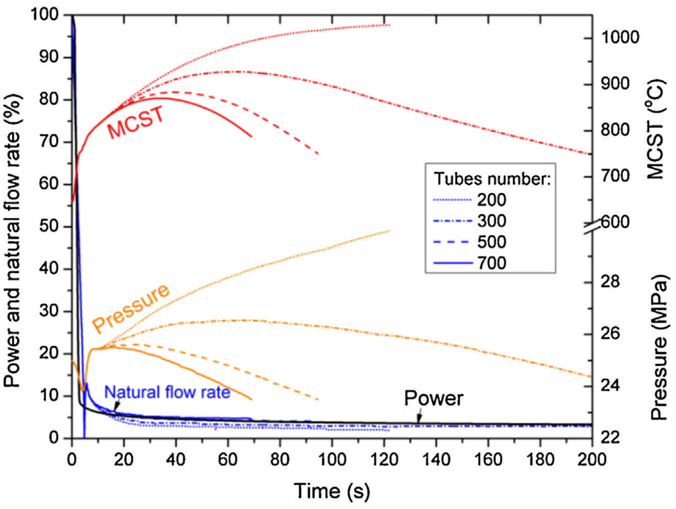

Fig. 8. Performance of IC at different tubes number.

Fig. 9 shows the performance of the IC as function of elevation of the IC. The height of downcomer is assumed to be 3 m. The total of hydrostatic pressure in the bottom part of the core will be due to both the elevation of IC and the height of downcomer. The calculation results show that elevation of 2 m leads to continuing increases of core pressure and MCST due to low natural flow rate. Elevation of 3 m and more than 3 m give high natural flow rates which can be used for mitigation of the pressure and the MCST.

When the pressure decrease achieves 23.5 MPa, the ADS is actuated. Calculation results of ADS operation in the Super FR are shown in Fig. 10. For simplification, this calculation assumes that the ADS is actuated by flow low 6% because operation of ADS is independent from the initial condition (Ishiwatari et al., 2005a). The core flow rate is induced largely leading to an effective mitigation of MCST. However, the coolant mass in the RPV is also decreased due to the ADS flow rate. When the pressure achieves saturation pressure of about 7 MPa, the ADS valves are closed and the remaining coolant mass in the RPV is used for heat removal at subcritical pressure by line switching to the IC. If the ADS valves are kept open, the coolant

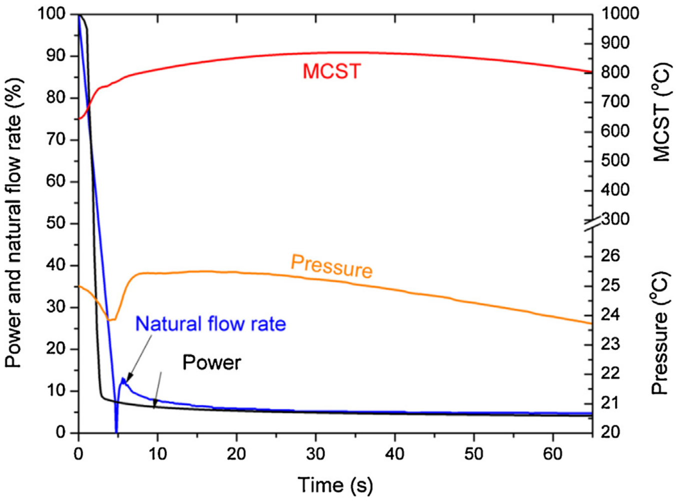

Fig. 7. Total loss of feedwater flow rate with IC at supercritical pressure.

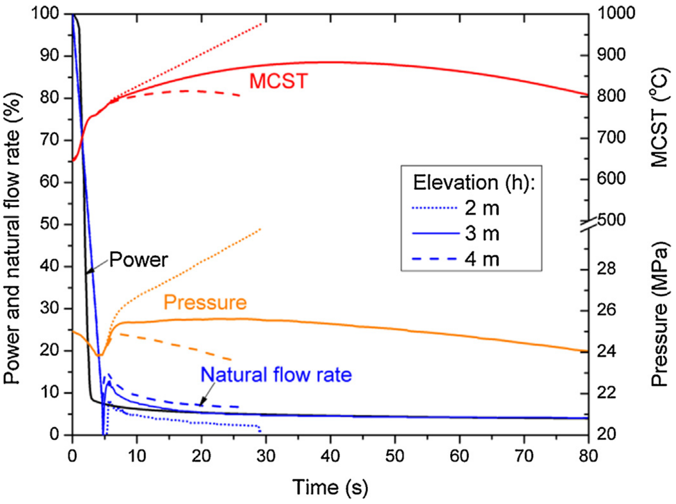

Fig. 9. Performance of IC as function of elevation.

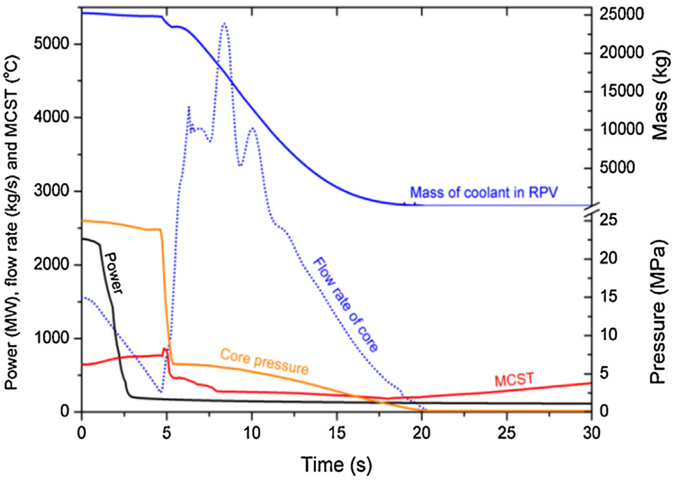

Fig. 10. ADS operation of the Super FR with single flow pass core.

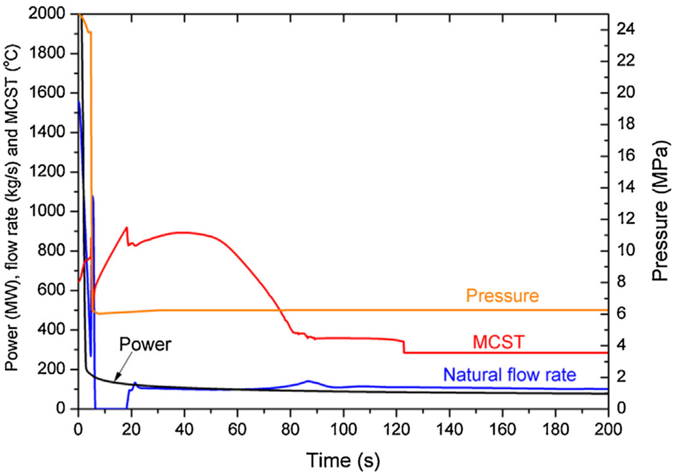

Fig. 11. Total loss of feedwater flow rate with IC at subcritical pressure.

mass, the pressure and the MCST will continue to decrease until the blow down is finished.

At subcritical pressure, the natural flow rate is calculated based on momentum balance equation. Steam flow rate from core to condenser tubes is calculated by Eq. (11) and condensate flow rate from condenser tubes to core is calculated by Eq. (12) (Khan and Rohatgi, 1992).

Steam flow rate:

$$V_{\text{steam}} = \sqrt{2\frac{\Delta P_{\text{RPV}} - z\rho_{\text{steam}}g}{\rho_{\text{steam}}(1+k)}} \tag{11}$$

Condensate flow rate:

$$V_{\text{liquid}} = \sqrt{2\frac{\Delta P_{\text{RET}} + z\rho_{\text{liquid}}g}{\rho_{\text{liquid}}(1+k)}} \tag{12}$$

ΔP_{RPV} is pressure difference between RPV and condenser tubes, while ΔP_{RET} is pressure difference between condenser tubes and the lower plenum. Parameter of k is pressure drop factor which is assumed conservatively to be 25. Pressure calculations in RPV and in condenser tubes are using ideal gas model as Eq. (13).

$$PV = \frac{m}{M}RT \tag{13}$$

where P is the pressure (Pa), V is volumes of core and condenser tubes containing steam (m^3), m is mass of steam (kg), T is steam temperature (°C), while parameters of M and R are molar mass and gas constant.

Calculation results of the IC performance after line switching are shown in Fig. 11. When the operation line is switched from ADS to IC lines, the natural flow rate cannot be immediately generated firstly due to low pressure difference between the condenser and the core and secondly due to low density difference between the condensate and the coolant in the core after the ADS operation. The MCST is suddenly increased due to loss of core flow rate caused by closing of ADS valves. However, condensation of steam in the condenser tubes leads to a lower pressure in the condenser tubes and produces more condensate in the drain line leading to higher hydrostatic pressure of the condensate. Finally the natural flow rate is generated within about 15 s from the line switching. Then the MCST is decreased to saturated temperature. The peak of the MCST is still below the criterion.

During the line switching from ADS to the IC, it is possible to use a CMT for coolant recovery. The CMT valve is opened automatically when the ADS valves are totally closed. Governing equations of the flow injection are mass conservation, Bernoulli equation, and Darcy formula as shown in Eqs. (14)–(16).

Mass conservation:

$$\rho_l A_{\text{tank}}\frac{\mathrm{d}L}{\mathrm{d}t} = -\dot{m}_{\text{inj}} \tag{14}$$

Bernoulli equation:

$$\frac{P_1}{\rho_l g} + z_1 + \frac{v_1^2}{2g} = \frac{P_2}{\rho_l g} + z_2 + \frac{v_2^2}{2g} + h_l \tag{15}$$

Darcy formula:

$$h_l = \frac{v_2^2}{2g}\left(\frac{fl}{\mathrm{d}}\right) \tag{16}$$

Variable of ρ_l is water density in the CMT (kg/m^3) which is assumed to be constant, L is the water level (m), A_{tank} is the area of CMT (m^2), $\dot{m}_{\text{inj}}$ is the outlet flow rate of the CMT (kg/s). Variables of P_1 and P_2 are pressures in the surface of water level in the CMT and in the outlet of CMT. Variable h_l is head loss of the pipe connecting the CMT and the RPV while parameter of l/d is ratio of length to diameter of the pipe. Parameter of f is coefficient of laminar flow.

Calculation results of using the CMT are shown in Fig. 12. Use of CMT drives early natural flow rate by coolant injection due to gravity force on the cold water in the CMT. The delay time of natural flow generation of IC is omitted and the increase of MCST is more mitigated. Besides, the coolant injection also acts as coolant recovery which increases the coolant mass in the RPV. Afterwards, the IC will act as long-term core cooling.

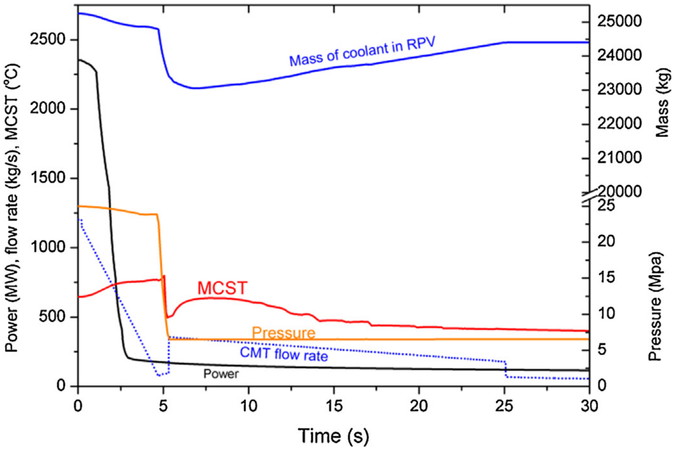

Fig. 12. Use of CMT for coolant recovery during line switching from ADS to IC lines.

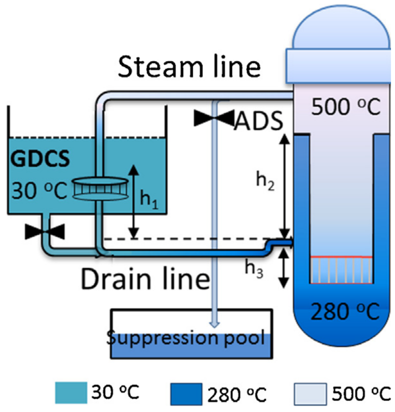

Fig. 13. Scheme of emergency condenser of a Super FR.

It is possible to remove the valves of IC leading to an online emergency condenser (EC) during the operation of the reactor (Zacharias et al., 2012). Fig. 13 shows the scheme of EC of the Super FR. GDCS is used as the condenser pool due to low position of the EC. At normal operation, the condenser tubes are filled with cold water of about 30 °C as shown by the height of h_1. This cold water will give hydrostatic pressure to the coolant in the downcomer (h_3) which the temperature is 280 °C. To compensate the hydrostatic pressure, h_2 of the downcomer which is above the connection of the drain line to the downcomer is provided. The height of h_2 must be longer than the height of h_1 due to lower water density in the downcomer. Based on the calculation results shown in Fig. 9, the minimum elevation of h_1 is 3 m. Fig. 14 shows the calculation results of EC at normal operation with 3 m of h_1 and the length of h_3 the same as the height of the core (2.4 m). Length of h_2 is varied to calculate the heat leakage during normal operation. From the operating principle, the total height of the downcomer should be long due to high hydrostatic pressure in the drain line. It is one disadvantage of using emergency condenser in a Super FR.

4.2.2. Loss of coolant accident (LOCA)

Large LOCA accident is analyzed in this study. Past study of safety analysis of the single flow pass core of Super FR showed that ADS was sensitive to be actuated in accidents of large LOCA due to less water inventory in the RPV. Large LOCA of 100% cold-leg break is the most severe accident of large LOCAs (Sutanto and Oka, 2014). Therefore, in this study the 100% cold-leg break of large LOCA accidents is analyzed. Fig. 15 shows the calculation results of the MCST during blowdown of 100% cold-leg break large LOCA of the single-flow pass core of Super FR. ADS valves are assumed to open 100% and the blowdown is finished at about 15 s. Within the first 15 s, the MCST is decreased due to large core flow rate induced by the ADS, while the pressure is also decreased to be the same as containment pressure, 0.15 MPa. After 15 s, the MCST starts increasing due to complete loss of coolant and flow rate. In the past study, LPCI was used for core reflooding which was actuated by pressure low 23.5 MPa with delay time of 30 s considering the startup time of the LPCI pumps (Ishiwatari et al., 2005a). For the first 8 s from its coolant injection, the LPCI flooded the lower plenum. Therefore the starting time of core reflooding was at about 38 s including the delay time (Sutanto and Oka, 2014).

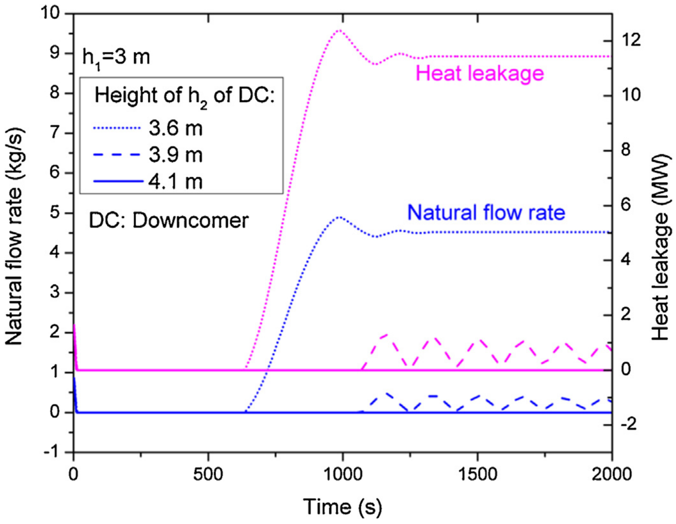

Fig. 14. Heat leakage of emergency condenser at normal operation.

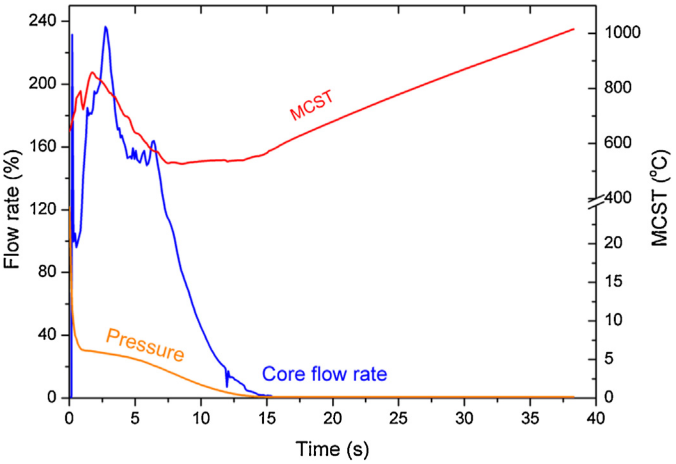

Fig. 15. Blowdown of 100% cold-leg break large LOCA of the single-flow pass core of Super FR (Sutanto and Oka, 2014).

In this study the LPCI is replaced by the GDCS. The GDCS starts reflooding when the core pressure is the same as containment pressure which is after 15 s. However, it is conservatively assumed to start reflooding at about 38 s the same as that of LPCI with assumption that the lower plenum is already filled of water. Outlet flow rate of the GDCS is calculated using the same way as that of the CMT. Driving force of the core reflooding is assumed only by hydrostatic pressure of water level in the downcomer. Core flow rate of reflooding will be the function of water level and pressure differences between the downcomer and the core. Pressure in the downcomer is assumed the same as containment pressure. Eq. (17) shows the momentum equation of the injection flow rate calculation.

$$\frac{dV_d}{dt}\times A_d\left[\frac{Z_d}{A_d}+\frac{Z_c}{A_c}+\frac{\mathrm{Vol}_{lp}}{A_{lp}^2}\right]=\frac{P_d-P_c}{\rho_f}+g_c\left(Z_d-Z_c\right)$$
$$-V_d\left|V_d\right|A_d^2\left(\frac{1}{A_c}-\frac{1}{A_d}\right)\left(\frac{1}{A_{lp}}+\frac{1}{2A_c}+\frac{1}{2A_d}\right) \qquad (17)$$

where V is coolant velocity (m/s), A is area (m^2), Z is water level (m), P is pressure (Pa) and g is conversion factor. Subscripts of d, c, lp, up, and f mean downcomer, core, lower plenum, upper plenum, and liquid, respectively.

Calculation results of the GDCS and the core flow rates are shown in Figs. 16 and 17. At the beginning, the flow rate of GDCS is used for filling the downcomer while core reflooding is started due to the water level difference. High flow rate of GDCS leads to fast increase of water level in the downcomer. After the water level achieves the top of the downcomer, it is assumed conservatively that the GDCS flow will just keep the water level of the downcomer as shown by rapid decrease of the GDCS flow rate. Meanwhile, core flooding is slow at the beginning due to high rate of vaporization in the core

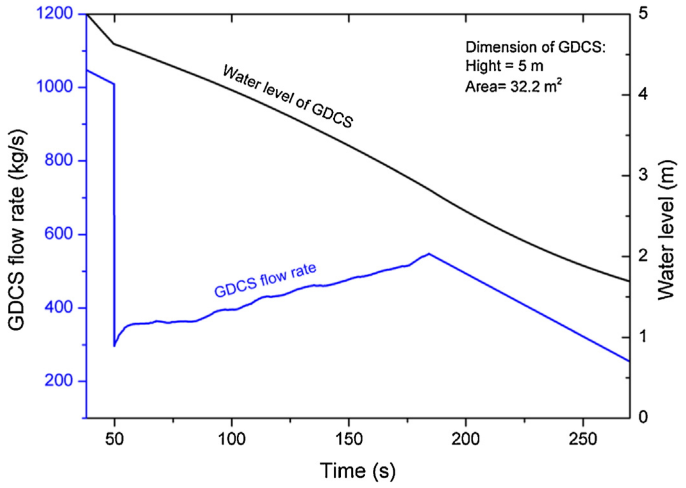

Fig. 16. Outlet flow rate of GDCS.

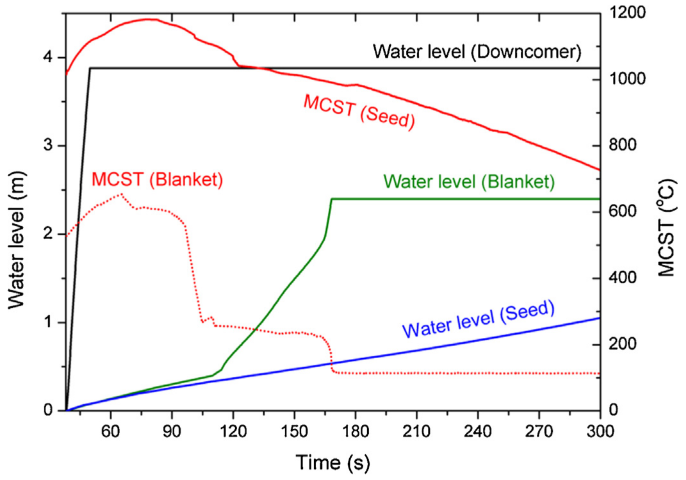

Fig. 17. MCST during reflooding by GDCS.

caused by high power peaking at the bottom part of the core. After the core water level achieves about 0.5 m, the water level in the blanket assembly increases rapidly, while that of seed assembly is still low due to higher decay power. The peak of MCST occurs at about 0.25 m of core water level and it still satisfies the criterion. Afterwards the MCST decreases slightly. After the reflooding is finished, vaporization is still continuing due to the remaining decay heat. The vapor will be released to containment and the PCCS will condensate the vapor and flow it to the GDCS by gravity. So that, long term cooling by the GDCS and the PCCS can be kept.

5. Conclusion

Passive safety system of a Super Fast Reactor has been studied. The passive system consists of isolation condenser (IC), automatic depressurization system (ADS), core make-up tank (CMT), gravity driven cooling system (GDCS) and passive containment cooling system (PCCS). Two accidents of total loss of feedwater flow and 100% cold-leg break of large LOCA are analyzed by using the passive system and the criteria of MCST and pressure are satisfied. The passive systems of IC, ADS, and CMT can be used for mitigation of the total loss of feedwater flow accident. High hydrostatic pressure of cold water in the drain line leads to early natural flow generation at supercritical pressure which removes the decay heat. Decreased pressure due to the heat removal actuates the ADS which enhances the MCST mitigation. At subcritical pressure, heat removal by natural circulation of IC is continued by line switching from ADS to IC. Use of CMT recovers the loss of coolant due to ADS operation. In case of large LOCA, GDCS can be used for reflooding of 100% cold-leg break LOCA. The MCST satisfies the criterion.

Acknowledgments

The first author, Sutanto, is grateful to Dr. Triwulan Tjiptono for supporting this study. The first author also acknowledges firstly the graduate scholarship from Ministry of Research and Technology, Republic of Indonesia, and second the Institution of National Nuclear Energy Agency of Indonesia for the permission of doing the study.

References

Cao, L., Oka, Y., Ishiwatari, Y., Shang, Z., 2008. Fuel, core design and subchannel analysis of a super fast reactor. J. Nucl. Sci. Technol. 45 (2), 138–148.

Cummins, W.E., Corletti, M.M., Schulz, T.L., 2003. Westinghouse AP1000 advanced passive plant. In: Proceeding of ICAPP '03, May 4–7, 2003, Cordoba, Spain (paper no. 3235).

Ikejiri, S., Ishiwatari, Y., Oka, Y., 2010. Safety analysis of supercritical-pressure water-cooled fast reactor under supercritical pressure. J. Nucl. Eng. Des. 240, 1218–1228.

Ishiwatari, Y., Oka, Y., Koshizuka, S., Yamaji, A., Liu, J., 2005a. Safety of super LWR, (I) safety system design. J. Nucl. Sci. Technol. 42 (11), 927–934.

Ishiwatari, Y., Oka, Y., Koshizuka, S., Yamaji, A., Liu, J., 2005b. Safety of super LWR, (II) safety analysis at supercritical pressure. J. Nucl. Sci. Technol. 42 (11), 935–948.

Kataoka, I., Ishii, M., 1984. Mechanistic modeling of pool entrainment phenomenon. Int. J. Heat Mass Transfer 27 (11), 1999–2014.

Khan, H.J., Rohatgi, U.S., 1992. Performance Characterization of Isolation Condenser of SBWR. Brookhaven National Laboratory, Upton, NY 11973 (Master Thesis).

Li, H., Oka, Y., Ishiwatari, Y., 2013. Safety analysis of a supercritical water cooled fast reactor with all-upward two-pass flow. J. Ann. Nucl. Energy 59, 1–9.

Liu, Q., Oka, Y., 2013a. Core design for super fast reactor with all upward flow core cooling. J. Ann. Nucl. Energy 57, 221–229.

Liu, Q., Oka, Y., 2013b. One-Pass Core Design of a Super Fast Reactor. GLOBAL, Salt Lake City, UT (September 29–October 3).

Liu, Q., Oka, Y., 2015. Single pass core design for a super fast reactor. J. Ann. Nucl. Energy 80, 451–459.

MacDonald, P., Buongiorno, J., Sterbentz, J.W., Davis, C., Witt, R., 2005. Feasibility Study of Supercritical Light Water Cooled Reactors for Electric Power Production, Final Report. Idaho National Engineering and Environmental Laboratory Bechtel BWXT Idaho, LLC, USA.

Oka, Y., Koshizuka, S., Ishiwatari, Y., Yamaji, A., 2010. Super Light Water Reactors and Super Fast Reactors. Springer, New York, NY.

Oka, Y., Morooka, S., Yamakawa, M., Ishiwatari, Y., Ikejiri, S., Katsumura, Y., Muroya, Y., Terai, T., Sasaki, K., Mori, H., Hamamoto, Y., Okumura, K., Kugo, T., Nakatsuka, T., Ezato, K., Akasaka, N., Hotta, A., 2011. Research and development of super light water reactors and super fast reactors in Japan. In: Proc. of ISSCWR-5, March 13–16, Vancouver, British Columbia.

Oka, Y., Jevremovic, T., 1996. Negative coolant void reactivity in large fast breeder reactors with hydrogenous moderator layer. Ann. Nucl. Energy 23, 1105–1115.

Okano, Y., Koshizuka, S., Kitoh, K., Oka, Y., 1996. Flow-induced accident and transient analyses of a direct-cycle, light-water-cooled, fast breeder reactor operating at supercritical pressure. J. Nucl. Sci. Technol. 33, 307–315.

Sutanto, Oka, Y., 2014. Accidents and transients analysis of a super fast reactor with single flow pass core. J. Nuclear Eng. Des. 273, 165–174.

Wu, P., Gou, J., Shan, J., Jiang, Y., Zhang, B., 2012. LOFA and LOCA analysis on CGNPC SCWR. In: Proceeding of ICAPP'12, June 24–28, Chichago, USA, 2012 (paper no. 12443).

Xu, Y., Ishii, M., Feltus, M.A., 2004. Safety analysis of multiple-failure of passive safety system in SBWR-1200 SBLOCA. Nucl. Eng. Des. 230, 107–119.

Xu, W., Cai, J., Liu, S., Tang, Q., 2015. Analysis of the influences of thermal correlations on neutronic-thermohydraulic coupling calculation of SCWR. Nucl. Eng. Des. 284, 50–59.

Yoo, J., Ishiwatari, Y., Oka, Y., Liu, J., 2006. Conceptual design of compact supercritical water-cooled fast reactor with thermal hydraulic coupling. Ann. Nucl. Energy 33, 945–956.

Zacharias, T., Novotny, C., Bielor, E., 2012. KERENA safety concept in the context of the Fukushima accident. In: Proceeding of ICAPP'12, June 24–28, Chicago, USA, 2012 (paper no. 12366).

Zhu, D., Tian, W., Zhao, H., et al., 2013. Comparative study of transient thermal–hydraulic characteristics of SCWRs with different core design. Ann. Nucl. Energy 51, 135–145.